Norbisabolane and bisabolane sesquiterpenoids from the seeds of *Angelica keiskei*

Shinji Ohta [a,*], Yasunori Yuasa [a], Nobuwa Aoki [b], Emi Ohta [a], Tatsuo Nehira [a], Hisashi Ômura [a], Mylene M. Uy [c]

[a] *Graduate School of Integrated Sciences for Life, Hiroshima University, 1-7-1 Kagamiyama, Higashi-Hiroshima 739-8521, Japan*

[b] *Nagahama Institute of Bio-Science and Technology, 1266 Tamura-cho, Nagahama, Shiga 526-0829, Japan*

[c] *Department of Chemistry, Mindanao State University-Iligan Institute of Technology, Iligan City 9200, Philippines*

* Corresponding author. Tel.: +81-82-424-6537; fax: +81-82-424-0758.

E-mail address: ohta@hiroshima-u.ac.jp (S. Ohta)

Declarations of interest: none.

ABSTRACT

A norbisabolane-type sesquiterpenoid, ashitabaol B and two bisabolane-type sesquiterpenoids, ashitabaols C and D, were isolated together with known sesquiterpenoids, ashitabaol A and (+)-bisabolangelone, from the seeds of *Angelica keiskei* (Miq.) Koidz. The structures including absolute configuration were determined on the basis of their spectroscopy, X-ray crystallography, and chemical conversions.

Keywords: Angelica keiskei (Miq.) Koidz.; Apiaceae; Ashitabaol A–D; Bisabolangelone; Bisabolane sesquiterpenoid.

1. Introduction

An excessive generation of free radicals causes damage to intracellular and extracellular proteins, polyunsaturated fatty acids, and nucleic acids (Tabata et al., 2010). The seed germination process involves the initiation of respiration and imbibition. Free radicals are continuously produced during the seed germination process and cause the seed tissue to be at the risk of oxidative damage. It has been reported that seeds have the ability to protect tissue against oxidative injury (Bailly et al., 2008). The capacity for scavenging free radicals increases significantly during germination (Lopez-Amoros et al., 2006). In the course of our search for antioxidants from the Japanese herb *Angelica keiskei* (Miq.) Koidz. (Japanese name "Ashitaba"), we found that the methanolic extract of the seeds of *A. keiskei* exhibited potent free radical scavenging activity. A preliminary examination of the active extract led to the isolation of an undescribed bisabolane-type sesquiterpenoid designated ashitabaol A (**4**) (Aoki and Ohta, 2010). However, the absolute configuration of **4** remains to be elucidated. Further investigation of the extract resulted in the isolation of three undescribed compounds designated ashitabaols B (**1**), C (**2**), and D (**3**) as well as the known bisabolane-type sesquiterpenoid, (+)-bisabolangelone (**5**) (Novotny et al., 1966) (Fig. 1). (+)-Bisabolangelone (synonym: ligustilone) (**5**) has been reported to exhibit many biological and pharmacological activities, including anti-ulcer (Wang et al., 2009), acaricidal (Kang et al., 2006), cytotoxic (Bae et al., 1994), antifeedant (Benz et al., 1989; Nawrot et al., 1984; Muckensturm et al., 1981), anti-inflammatory (Jung et al., 2010; Kim et al., 2013), and inhibitory activity against pig gastric H^+/K^+-ATPase (Luo et al., 2012) and melanogenesis (Lee et al., 2012). Its absolute configuration was originally assigned as 1*R*,6*S*,7*S* (**5'**) based

upon a comparison of its ECD spectrum with those of ponasterons A–C by Yu et al. (1995). However, the structure of (+)-bisabolangelone is considerably different from those of ponasterons A–C and its absolute configuration has been stated as 1*S*,6*R*,7*R* (**5**) via the synthesis of TMS-*ent*-bisabolangelone by Riss et al. (2017), suggesting the need for a reexamination of the absolute configuration. In this report, we describe the isolation and structural elucidation of undescribed compounds **1**–**3**, the determination of absolute configurations of ashitabaol A (**4**) and (+)-bisabolangelone (**5**) using X-ray crystallography, the chemical conversion of ashitabaol A (**4**) and (+)-bisabolangelone (**5**) to compounds **1**–**3**, and the antioxidant activity of the isolated sesquiterpenoids.

2. Results and discussion

The methanolic extract of the seeds of *A. keiskei* was partitioned between *n*-hexane and H_2O and the aqueous layer was extracted with EtOAc. The *n*-hexane-soluble portion was subjected to repeated separation on a silica gel column to afford **4** and **5**. On the other hand, the EtOAc-soluble portion was subjected to silica gel column chromatography (CC) followed by purification by silica gel CC or octadecylsilyl (ODS) CC to afford **1** and **3**. The H_2O-soluble portion was subjected to ODS CC followed by purification by silica gel CC and ODS CC to yield **2** and **3**, respectively.

Compound **1** was obtained as colorless crystals (m.p. 114.0–114.5 ˚C from CH_2Cl_2–*n*-hexane). The molecular formula of **1** was determined to be $C_{12}H_{16}O_3$ on the basis of the positive-ion HRESITOFMS data (*m/z* 209.1172 $[M+H]^+$; calcd for $C_{12}H_{17}O_3^+$, 209.1172), indicating five degrees of unsaturation. The IR spectrum displayed absorption bands at 3385 (OH), 1636, and 1624 cm^{-1}

(C=C). The UV (MeOH) absorption maximum observed at 271 nm (log ε 4.11) indicated the presence of conjugated double bonds. The ^{1}H and ^{13}C NMR (Table 1) of **1** were similar to those of ashitabaol A (**4**) (Aoki and Ohta, 2010) except for resonances of the side chain. HMBC correlations between the aldehyde proton signal observed at δ_H 9.89 (H-10) and C-9; the olefinic proton signal at δ_H 5.31 (H-9) and C-8; and the methyl proton signal at δ_H 1.56 (H_3-11) and C-6, C-7, and C-8, demonstrated the attachment of the formylmethylidene unit at C-8 in the hexahydrobenzofuran skeleton of **1**. The relative configuration of **1** was established using coupling-constant analysis and NOESY data. The NOESY correlations observed between H-1, H-6, and H_3-11 and the small vicinal coupling ($^{3}J_{H1\text{-}H6}$ = 4.6 Hz) observed between H-1 and H-6 indicated the presence of a *cis*-fused hexahydrobenzofuran ring. In addition, the NOESY correlation observed between H-9 and H_3-11 indicated the geometry of the C=C double bond between C-8 and C-9 was *Z* (Fig. 2). The structure of **1** was confirmed using X-ray crystallography (Fig. 3). Consequently, the structure of **1** was established as shown in Fig. 1. This compound was named ashitabaol B.

The molecular formula of compound **2** was established to be $C_{15}H_{24}O_4$ on the basis of the positive-ion HRESIFTMS data (*m/z* 291.1568 $[M+Na]^+$; calcd for $C_{15}H_{24}O_4Na^+$, 291.1567), indicating four degrees of unsaturation. The IR spectrum displayed absorption bands at 3390 (OH), 1684, and 1626 cm^{-1} (C=O and C=C). The UV (MeOH) absorption maxima observed at 231 (log ε 3.43) and 330 nm (log ε 2.54) indicated the presence of conjugated double bonds. The ^{1}H NMR, ^{13}C NMR (Table 1), and HSQC data of **2** revealed the presence of four aliphatic methyls (δ_H 1.27, 1.38, 1.39, and 1.40; δ_C 22.5, 29.2, 29.3, and 29.5), two aliphatic methylenes (δ_H 1.55, 1.72, 1.85, and 1.86; δ_C 19.0 and 36.6), an

aliphatic methine (δ_H 2.48; δ_C 42.7), four sp^2 methines (δ_H 5.36, 5.78, 6.69, and 7.16; δ_C 119.0, 128.5, 136.4, and 155.9), three oxygenated quaternary carbons (δ_C 66.7, 71.2, and 79.6), and a carbonyl carbon (δ_C 202.7). Interpretation of the ^1H–^1H COSY data led to two proton spin network systems, H-2/H-1/H-6/H_2-5/H_2-4 and H-9/H-10 (Fig. 2). The HMBC correlations observed between H_3-15 and C-2, C-3, and C-4; H_3-14 and C-6, C-7, and C-8; H-9 and C-8 and C-11; H-10 and C-8 and C-11; and H_3-12 and H_3-13 with C-10 and C-11 revealed the presence of a bisabolane skeleton (Fig. 2). The ^{13}C NMR chemical shifts of C-3 (δ_C 66.7), C-7 (δ_C 79.6), and C-11 (δ_C 71.2) indicated the attachment of a hydroxyl group to each position, leading to the gross structure of **2**. The large vicinal coupling constants of 13.1 Hz observed between H-4β and H-5α, and 10.1 Hz between H-5α and H-6 indicated that these protons occupy axial or pseudoaxial positions (Fig. S1). Further, the NOESY correlation observed between H_3-15 and H-4β indicated the relative configuration of the cyclohexene ring in **2** as shown in Fig. S1. The *E*-geometry of Δ^9 was determined by the large vicinal coupling constant of 15.3 Hz observed between H-9 and H-10. Consequently, the structure of **2** was established as shown in Fig. 1. This compound was named ashitabaol C.

In a preliminary experiment, compound **3** underwent decomposition in MeOH. The ^1H NMR spectrum of the decomposition product showed the presence of an additional methoxyl signal, suggesting the conversion of **3** into an acetal derivative in the presence of an alcoholic solvent. Thus, the spectroscopic data obtained for **3** were collected in an aprotic solvent ($CHCl_3$ or $CDCl_3$). The molecular formula of **3** was established to be $C_{15}H_{22}O_5$ on the basis of the positive-ion HRESIFTMS data (*m/z* 305.1361 $[M+Na]^+$; calcd for $C_{15}H_{22}O_5Na^+$,

305.1359), indicating five degrees of unsaturation. The IR spectrum displayed absorption bands at 3393 (OH) and 1644 cm^{-1} (C=O and C=C). The UV ($CHCl_3$) absorption maximum observed at 325 nm (log ε 2.18) indicated the presence of conjugated double bonds. The ^1H NMR, ^{13}C NMR (Table 1), and HSQC data of **3** revealed the presence of three aliphatic methyls (δ_H 1.40, 1.41, and 1.43; δ_C 22.4, 29.2, and 29.3), an olefinic methyl (δ_H 2.03; δ_C 24.8), an aliphatic methylene (δ_H 2.60 and 2.67; δ_C 40.4), an aliphatic methine (δ_H 2.84; δ_C 62.7), an oxygenated methine (δ_H 4.52; δ_C 66.3), three sp^2 methines (δ_H 5.97, 7.11, and 7.19; δ_C 119.7, 125.6, and 156.7), two oxygenated quaternary carbons (δ_C 71.3 and 80.3), an sp^2 quaternary carbon (δ_C 161.2), and two carbonyl carbons (δ_C 199.0 and 207.1). Interpretation of the ^1H–^1H COSY data led to two proton spin network systems, H-4/H-5/H-6 and H-9/H-10 (Fig. 2). HMBC correlations observed between H-2 and C-4 and C-15; H-4 and C-2 and C-3; H_3-15 and C-2, C-3, and C-4; H-6 and C-1 and C-7; H_3-14 and C-6, C-7, and C-8; H-9 and C-8 and C-11; H-10 and C-8 and C-11; and H_3-12 and H_3-13 with C-10 and C-11 revealed the gross structure of **3** (Fig. 2). The appearance of a quartet proton signal for H-5 with a very small vicinal coupling constant (J = 2.7 Hz) indicated that H-5 and 5-OH occupy equatorial and axial positions, respectively, and that H-5 and H-6 are arranged in a *cis* manner. The relative configuration of the cyclohexene ring of **3** was supported by the NOESY correlation observed between H-5 and H-6 as shown in Fig. 2. The *E*-geometry of Δ^9 was determined by the large vicinal coupling constant of 15.6 Hz observed between H-9 and H-10. Consequently, the structure of **3** was established as shown in Fig. 1. This compound was named ashitabaol D.

Although the relative configuration of ashitabaol A (**4**) has been elucidated by X-ray crystallography using Mo Kα radiation (Aoki and Ohta,

2010), the absolute configuration remained unsolved. In the present study, ashitabaol A (**4**) was treated with *p*-bromobenzoic anhydride to afford its 7-*p*-bromobenzoate derivative (**6**). The ECD spectrum of **6** exhibited a negative first Cotton effect at 257 nm and a positive second Cotton effect at 239 nm, indicating that **6** has negative exciton chirality (Fig. S2). These findings indicated that the electric transition moments of the two chromophores of the C-7 benzoate and C-8 diene constitute a left-handed helicity. Thus, the absolute configuration of ashitabaol A (**4**) was determined to be 1*S*,6*R*,7*R*, which was unambiguously confirmed by X-ray crystallography using the anomalous scattering of Cu Kα radiation with the Flack parameter (Parsons and Flack, 2004; Parsons et al., 2013) being refined to 0.1 (1) (Fig. 3).

Compound **5** was obtained as colourless crystals (CH_2Cl_2–*n*-hexane). The molecular formula of **5** was established to be $C_{15}H_{20}O_3$ on the basis of the positive-ion HRESITOFMS data (*m/z* 271.1304 $[M+Na]^+$, calcd for $C_{15}H_{20}O_3Na^+$, 271.1305). The melting point, specific optical rotation, and spectroscopic data (UV, IR, ^{1}H NMR, and ^{13}C NMR) of **5** were in good accordance with those of (+)-bisabolangelone described in the literature (Riss et al., 1989; Bae et al., 1994; Yu et al., 1995; Kang et al., 2006), indicating that both compounds were the same. The absolute configuration of (+)-bisabolangelone was originally assigned as 1*R*,6*S*,7*S* (**5'**) based upon a comparison of its ECD spectrum with those of ponasterons A–C (Yu et al. 1995). However, Riss et al. (2017) have stated the absolute configuration of (+)-bisabolangelone as 1*S*,6*R*,7*R* (**5**) via the synthesis of TMS-*ent*-bisabolangelone. In the present study, the absolute configuration of (+)-bisabolangelone was reexamined and confirmed unambiguously as 1*S*,6*R*,7*R* (**5**) by X-ray crystallography using the anomalous scattering of Cu Kα radiation

with the Flack parameter (Parsons and Flack, 2004; Parsons et al., 2013) being refined to 0.07 (3) (Fig. 3).

Ashitabaol A (**4**) exhibited 2,2'-azinobis(3-ethylbenzothiazoline-6-sulfonic acid) (ABTS) free radical scavenging activity with SC_{50} = 13.8 μM (Aoki and Ohta, 2010). However, compounds **1**–**3** and (+)-bisabolangelone (**5**) did not exhibit ABTS free radical scavenging activity even at a concentration of 100 μM.

The reactivity of ashitabaol A (**4**) was further evaluated against selected reactive oxygen species such as superoxide radicals, hydrogen peroxide, hydroxyl radicals, and singlet oxygen. Ashitabaol A (**4**) at a concentration of 100 μM did not react with superoxide radicals or hydrogen peroxide, but did show activity against the hydroxyl radicals (SC_{50} = 60.4 μM). Furthermore, reaction of **4** with singlet oxygen generated via irradiation of visible light (>475 nm) in the presence of rose bengal was monitored using spectrophotometry (Fig. S3). As the reaction progressed, the absorption band of **4** observed at 257 nm decreased, indicating that **4** was gradually decomposed upon attack by singlet oxygen. The reaction was also monitored using ^{1}H NMR spectroscopy. The ^{1}H NMR spectra of **4** in the presence of rose bengal were recorded after irradiation of light (>475 nm) for 0–60 min (Fig. S4). After 10 min of light irradiation, two doublet proton signals appeared at δ_H 9.8 and 5.7. These signals were attributed to a formylmethylidene structure in the product, implying the production of ashitabaol B (**1**). The UV, ^{1}H NMR, ESIMS, and ECD spectra of the purified major product were identical to those of natural ashitabaol B (**1**), supporting the conversion of **4** into **1** by singlet oxygen and confirmed the absolute configuration of **1** as 1*S*,6*R*,7*R*. Although several light-sensitive natural compounds such as coumarins and flavones have

been reported, one of the most potent is chlorophyll (Knox and Dodge, 1985). In fact, when visible light was irradiated onto a MeOH solution of the crude extract of the seeds of *A. keiskei,* a significant decrease in the ashitabaol A (**4**) content was observed during HPLC analysis. Moreover, the UV-Vis spectrum of the crude extract showed the presence of trace amounts of chlorophylls a and b. As the germination of *A. keiskei* seeds requires light irradiation, singlet oxygen can be generated on the seed coat containing a trace amont of chlorophylls a and b. Several diene compounds have been reported to give aldehyde products upon reaction with singlet oxygen via a dioxetane intermediate (Gollnick and Griesbeck, 1984; Matsumoto et al., 1985; Clennan, 1991; Murthy et al., 2009). These observations indicated that ashitabaol A (**4**) was oxidized by singlet oxygen to produce ashitabaol B (**1**) via a dioxetane intermediate in *A. keiskei* seeds, as shown in Fig. 4.

Compounds **4** and **5** were oxidized using Fenton's reagent. The UV, ^{1}H NMR, ESIMS, and ECD spectra of the purified products derived from **4** and **5** were identical to those of natural ashitabaol C (**2**) and ashitabaol D (**3**), respectively. Thus, the absolute configurations of **2** and **3** were determined as shown in Fig. 1. As hydroxyl radicals have been reported to be formed from H_2O_2 either non-enzymatically via the Fenton reaction (Kuchitsu et al., 1995; Fry, 1998) or enzymatically via peroxidases (Schweikert et al., 2000; Schopfer et al., 2001; Liszkay et al., 2003) during desiccation, germination, and seedling growth of several plant seeds (Karkonen and Kuchitsu, 2015), ashitabaol C (**2**) and ashitabaol D (**3**) can be produced from ashitabaol A (**4**) and (+)-bisabolangelone (**5**) by hydroxyl radicals generated in the seeds of *A. keiskei* as shown in Figs. 5A and 5C, respectively. However, in view of the stereoselectivity, the formation of

an epoxide intermediate by any enzymes, e.g., cytochrome P450, may be involved in the biogenetic formation of **2** and **3** as shown in Figs. 5B and 5D, respectively (Gesell et al., 2015; Mak and Denisov, 2018; Dezvarei et al., 2018; Bathe and Tissier, 2019). Although the production of reactive oxygen species such as hydroxyl radicals is regarded as a detrimental process causing various symptoms of oxidative stress in plant metabolism, they serve useful physiological functions in pathogen defence and in the wall-loosening process underlying cell extension growth (Schweikert et al., 2002). Ashitabaol A (**4**) and (+)-bisabolangelone (**5**) may have an important function in the strict control of the amount of very reactive hydroxyl radicals produced in the seeds of *A. keiskei*.

3. Conclusions

Three undescribed compounds (**1**–**3**) have been isolated from the seeds of *A. keiskei* along with two known sesquiterpenoids (**4** and **5**). Their structures and absolute configurations were elucidated on the basis of their spectroscopy, X-ray crystallography and chemical conversion. Although many bisabolane-type sesquiterpenoids have been isolated from natural sources (Fraga, 2013), C12-norbisabolane sesquiterpenoids possessing a hexahydrobenzofuran skeleton containing an acrylaldehyde unit such as ashitabaol B (**1**) are extremely rare in nature. Also, ashitabaols C (**2**) and D (**3**) have a unique 2,6-dihydroxy-6-methyl-3-oxohept-4-en-2-yl side-chain. Although several triterpenes possessing such a side-chain, e.g., cucurbitacins (Melera et al., 1960; Chen et al., 2005; Graziose et al., 2013; Zhu et al., 2018), exist in plants, these are the first examples of naturally occurring sesquiterpenoids having such a structure. Although ashitabaol A (**4**) exhibited ABTS radical scavenging activity,

compounds **1**–**3** and (+)-bisabolangelone (**5**) did not show any activity. Compounds **1** and **2** were considered to be the oxidation products of ashitabaol A (**4**), while compound **3** is the product of (+)-bisabolangelone (**5**). Ashitabaol A (**4**) was found to be abundantly present in the seed coat throughout the seed germination process on the basis of HPLC analysis (Aoki and Ohta, 2010). These findings indicate that ashitabaol A (**4**) plays a key role in the protection of *A. keiskei* seeds against oxidative stress initiated by reactive oxygen species such as singlet oxygen and free radicals produced during maturation, desiccation, and germination of the seeds.

4. Experimental

4.1. General experimental procedures

Melting point was recorded using a Round Science RFS 10 melting point apparatus. Optical rotations were measured on a JASCO P-2200 polarimeter. IR spectra were recorded using a JASCO FT/IR-6300 spectrometer. UV spectra were obtained using a JASCO V-630 spectrometer. ECD spectra were measured using a JASCO J-725 spectropolarimeter. NMR spectra were acquired using a JEOL A400 spectrometer (400 MHz for ^{1}H, 100 MHz for ^{13}C). ^{1}H and ^{13}C NMR chemical shifts were referenced to residual solvent peaks: δ_H 7.26 (residual $CHCl_3$) and δ_C 77.0 for $CDCl_3$. HRESITOFMS were carried out using a Shimadzu LCMS-IT-TOF mass spectrometer. HRESIFTMS were measured on a Thermo Fisher Scientific LTQ Orbitrap XL mass spectrometer at the Natural Science Center for Basic Research and Development (N-BARD), Hiroshima University. Column chromatography (CC) was performed using silica gel 60 (40 – 63 μm, Merck) and Wakogel 50C18 (Wako Pure Chemical Industries, Ltd, Osaka, Japan).

Thin layer chromatography (TLC) was performed using pre-coated silica gel 60 F_{254} plates (Merck) and pre-coated silica gel RP-18 F_{254}s plates (Merck).

4.2. Plant material

The seeds of *Angelica keiskei* (Miq.) Koidz. were purchased from Nishino-Farm (Tokyo, Japan) in January 2015, and identified as described in the literature (Aoki and Ohta, 2010). A voucher specimen has been deposited at the Hiroshima University Museum, Japan (registry number HUM-PL-00006).

4.3. Extraction and isolation

The seeds (589 g) of *A. keiskei* were extracted with acetone. The concentrated acetone extract (16 g) was suspended in water and then partitioned successively with *n*-hexane and EtOAc. A portion (3.5 g) of the *n*-hexane-soluble material (13 g) was subjected to silica gel CC eluted with EtOAc–*n*-hexane (0:100, 1:19, 1:9, 1:4, 3:7, 2:3, 1:1, 3:2, 7:3, 4:1, 9:1, 100:0) to obtain 12 fractions. The fractions eluted with EtOAc–*n*-hexane (1:19 and 1:4) yielded **4** (44 mg) and **5** (32 mg), respectively, upon recrystallization from CH_2Cl_2–*n*-hexane. The EtOAc-soluble portion (2.2 g) was subjected to silica gel CC eluted with acetone–*n*-hexane (0:100, 1:9, 1:4, 3:7, 2:3, 1:1, 3:2, 7:3, 4:1, 9:1, 100:0) to obtain 11 fractions. The fraction eluted with acetone–*n*-hexane (1:4) (56 mg) was purified by silica gel CC with EtOAc–*n*-hexane (0:100 to 1:4) to afford **1** (5 mg). The fraction eluted with acetone–*n*-hexane (3:7) (36 mg) was purified by ODS CC with acetone–H_2O (0:100 to 1:4) to afford **3** (9 mg). The H_2O-soluble portion (0.53 g) was subjected to ODS CC eluted with acetone–H_2O (0:100, 1:19, 1:9, 1:4, 3:7, 2:3, 1:1, 3:2, 7:3, 4:1, 9:1, 100:0) to obtain 12 fractions. The fraction eluted

with acetone–H_2O (1:9) (41 mg) was purified by silica gel CC with acetone–*n*-hexane (0:100 to 100:0) to afford **3** (10 mg). The fraction eluted with acetone–H_2O (1:4) (36 mg) was purified by ODS CC with acetone–H_2O (0:100 to 100:0) to afford **2** (5 mg).

*4.4. Ashitabaol B (**1**)*

Colorless crystals; m.p. 114.0–114.5 ˚C; $[\alpha]_D^{25}$ +166˚ (*c* 0.16, $CHCl_3$); UV (MeOH) λ_{max} (log ε) 271 nm (4.11); ECD (MeOH) $\Delta\varepsilon_{268}$ +29.9; IR (KBr) 3385 (OH), 1636, 1624 cm^{-1} (C=O and C=C); ^1H NMR and ^{13}C NMR spectroscopic data, see Table 1; HRESITOFMS *m/z* 209.1172 $[M+H]^+$ (calcd for $C_{12}H_{17}O_3^+$, 209.1172).

*4.5. X-ray crystallographic analysis of **1***

Data collection was performed with a Bruker SMART-APEX II ULTRA CCD area detector with graphite monochromated Mo Kα radiation (λ = 0.71073 Å). The structure was solved by direct methods using SHELXS-97 (Sheldrick 1997). Refinements were performed with SHELXL-2014/6 (Sheldrick, 2014) using full-matrix least squares on F^2. All non-hydrogen atoms were refined anisotropically. All hydrogen atoms were placed in idealized positions and refined as riding atoms isotropically. Crystal data: $C_{12}H_{16}O_3$, M = 208.25, orthorhombic, crystal size, 0.50 x 0.30 x 0.20 mm^3, space group $P2_12_12_1$, Z = 8, crystal cell parameters a = 7.9450 (6) Å, b = 9.8138 (7) Å, c = 28.851 (2) Å, V = 2249.5 (3) $Å^3$, F(000) = 896, Dc = 1.230 Mg/m^3, T = 173 K, 13613 reflections measured, 5318 independent reflections [$R_{(int)}$ = 0.0461], final R indices [$I>2.0\sigma(I)$], R_1 = 0.0460, wR_2 = 0.1221, final R indices (all data), R_1 = 0.0490, wR_2 = 0.1239.

CCDC-1918746 contains the supplementary crystallographic data for this paper. The data can be obtained free of charge from The Cambridge Crystallographic Data Centre via www.ccdc.cam.ac.uk/data_request/cif.

*4.6. Ashitabaol C (**2**)*

Colorless viscous oil; $[\alpha]_D^{25}$ –18° (*c* 0.12, $CHCl_3$); UV (MeOH) λ_{max} (log ε) 231 (3.43), 330 nm (2.54); ECD (MeOH) $\Delta\varepsilon_{229}$ +0.44, $\Delta\varepsilon_{320}$ –0.01; IR (film) 3390 (OH), 1684, 1626 cm^{-1} (C=O and C=C); ^1H NMR and ^{13}C NMR spectroscopic data, see Table 1; HRESIFTMS *m/z* 291.1568 $[M+Na]^+$ (calcd for $C_{15}H_{24}O_4Na^+$, 291.1567).

*4.7. Ashitabaol D (**3**)*

Colorless viscous oil; $[\alpha]_D^{25}$ –96° (*c* 0.32, $CHCl_3$); UV ($CHCl_3$) λ_{max} (log ε) 325 nm (2.18); ECD ($CHCl_3$) $\Delta\varepsilon_{327}$ –0.88; IR (film) 3393 (OH), 1644 cm^{-1} (C=O and C=C); ^1H NMR and ^{13}C NMR spectroscopic data, see Table 1; HRESIFTMS *m/z* 305.1361 $[M+Na]^+$ (calcd for $C_{15}H_{22}O_5Na^+$, 305.1359).

*4.8. X-ray crystallographic analysis of **4***

Data collection was performed with a Bruker SMART-APEX II ULTRA CCD area detector with graphite monochromated Cu Kα radiation (λ = 1.54178 Å). The structure was solved by direct methods using SHELXS-97 (Sheldrick 1997). Refinements were performed with SHELXL-2013 (Sheldrick, 2013) using full-matrix least squares on F^2. All non-hydrogen atoms were refined anisotropically. All hydrogen atoms were placed in idealized positions and refined as riding atoms isotropically. Crystal data: $C_{15}H_{22}O_2$, M = 234.32, monoclinic,

crystal size, 0.40 x 0.10 x 0.10 mm^3, space group *C*2, *Z* = 12, crystal cell parameters *a* = 46.8411 (11) Å, *b* = 6.2348 (2) Å, *c* = 14.6174 (4) Å, β = 107.2750 (10)˚, *V* = 4076.4 (2) $Å^3$, *F*(000) = 1536, *Dc* = 1.145 Mg/m^3, T = 173 K, 96045 reflections measured, 7287 independent reflections [$R_{(int)}$ = 0.0351], final *R* indices [$I>2.0\sigma(I)$], R_1 = 0.0414, wR_2 = 0.0929; final *R* indices (all data), R_1 value = 0.0425, wR_2 = 0.0933, Flack parameter (Parsons and Flack, 2004): 0.09 (3). CCDC-1918747 contains the supplementary crystallographic data for this paper. The data can be obtained free of charge from The Cambridge Crystallographic Data Centre via www.ccdc.cam.ac.uk/data_request/cif.

*4.9. (+)-Bisabolangelone (**5**)*

Colorless plates; m.p. 148–149 ˚C; $[\alpha]_D^{25}$ +146.3˚ (*c* 0.53, MeOH); UV (MeOH) λ_{max} (log ε) 244 (4.28), 252sh (4.25), 320 nm (3.36); IR (KBr) 3343 (OH), 1641 cm^{-1} (C=O and C=C); ^{1}H NMR and ^{13}C NMR spectroscopic data, see Table 1; HRESITOFMS *m/z* 271.1304 $[M+Na]^+$ (calcd for $C_{15}H_{20}O_3Na^+$, 271.1305).

*4.10. X-ray crystallographic analysis of **5***

Data collection was performed with a Bruker SMART-APEX II ULTRA CCD area detector with graphite monochromated Cu Kα radiation (λ = 1.54178 Å). The structure was solved by direct methods using SHELXS-97 (Sheldrick 1997). Refinements were performed with SHELXL-2013 (Sheldrick, 2013) using full-matrix least squares on F^2. All non-hydrogen atoms were refined anisotropically. All hydrogen atoms were placed in idealized positions and refined as riding atoms isotropically. Crystal data: $C_{15}H_{20}O_3$, *M* = 248.31, orthorhombic,

crystal size, 0.40 x 0.40 x 0.05 mm^3, space group $P2_12_12_1$, Z = 4, crystal cell parameters a = 6.96614 (9) Å, b = 8.92936 (11) Å, c = 22.6230 (3) Å, V = 1407.22 (3) $Å^3$, $F(000)$ = 536, Dc = 1.172 Mg/m^3, T = 173 K, 9563 reflections measured, 2659 independent reflections [$R_{(int)}$ = 0.0135], final R indices [$I>2.0\sigma(I)$], R_1 = 0.0300, wR_2 = 0.0830; final R indices (all data), R_1 value = 0.0302, wR_2 = 0.0834, Flack parameter (Parsons and Flack, 2004): 0.07 (3). CCDC-1918748 contains the supplementary crystallographic data for this paper. The data can be obtained free of charge from The Cambridge Crystallographic Data Centre via www.ccdc.cam.ac.uk/data_request/cif.

4.11. Preparation of ***8***

To a solution of **4** (3 mg) in dry CH_2Cl_2 (0.1 mL) were added an excess of *p*-bromobenzoic anhydride (ca. 10 eqiv), 4-(*N,N*-dimethylamino)pyridine (DMAP; 10 equiv), and triethylamine (10 equiv). The resulting mixture was stirred at 40 ˚C for 6 h. H_2O (0.5 mL) was added to the reaction mixture and resulting biphasic solution was extracted with *n*-hexane. The *n*-hexane extract was purified by short silica gel column chromatography (EtOAc–*n*-hexane, 1:19) to afford **8** (0.4 mg).

4.12. p-Bromobenzoate ***8***

Colorless oil; UV (MeOH) λ_{max} (log ε) 245 (4.33), 266 nm (sh) (4.07); IR (film) 1722 (C=O), 1673, 1633 (C=C), 1590, 1485 cm^{-1} (aromatic ring); ^1H NMR ($CDCl_3$, 400 MHz) δ_H 4.59 (1H, br t, J = 4.8 Hz, H-1), 5.71 (1H, br s, H-2), 1.90 (2H, m, H-4), 1.29 (1H, m, H-5), 1.41 (1H, m, H-5), 2.65 (1H, dt, J = 13.2 and 4.8 Hz, H-6), 5.39 (1H, d, J = 11.4 Hz, H-9), 6.10 (1H, br d, J = 11.4 Hz, H-10), 1.79

(1H, br s, H-12), 1.76 (1H, br s, H-13), 1.81 (1H, s, H-14), 1.74 (1H, br s, H-15), 7.90 (1H, d, J = 8.4 Hz, H-3' and H-7'), 7.59 (1H, d, J = 8.4 Hz, H-4' and H-6'); EIMS *m/z* (rel. int. %) 416 (M^+, 3), 418 (M^+, 3), 200 (100), 202 (100); ECD (MeOH) $\Delta\varepsilon_{239}$ +14.4, $\Delta\varepsilon_{257}$ –6.1.

4.13. ABTS radical scavenging activity assay

The ABTS radical scavenging activity assay was based on a literature method (Zhu et al., 2009; Guedes et al., 2013) with slight modification. A stable stock solution of ABTS radical was prepared by mixing equal volumes of aqueous solutions of 14 mM ABTS diammonium salt and 4.9 mM potassium persulfate for 16 h in the dark at room temperature. The ABTS radical solution was diluted with EtOH to an absorbance of 0.700 ± 0.002 at 734 nm, and equilibrated at room temperature. After addition of 1.0 mL of the diluted ABTS radical solution to 10 μL of each sample in EtOH, the absorbance at 734 nm was recorded in the dark at room temperature for 6 min. Trolox (SC_{50} = 9.6 μM) was used as a standard. All experiments were performed in duplicate.

4.14. Hydroxyl radical scavenging assay

The hydroxyl radical scavenging assay was based on a literature method (Yu et al., 2008) with slight modification. Samples were dissolved in 50 mM cetyltrimethyl ammonium bromide (CTAB) and serially diluted to the corresponding concentrations. A mixture of sample solution (100 μL), 0.2 mM rhodamine B (50 μL), 10 mM iron (II) sulfate (100 μL), 135 mM acetic acid (148 μL), 20 mM H_2O_2 (100 μL) and H_2O (502 μL), pH 2.8, in a microtube was incubated for 10 min at room temperature. The absorbance of rhodamine B was

measured at 550 nm. Trolox (SC_{50} = 92.8 μM) was used as a standard. All experiments were performed in duplicate.

*4.15. Conversion of **4** into **1**.*

Photolysis of **4** with singlet oxygen was performed using a literature method (Agon et al., 2006) with slight modification. Briefly, compound **4** (1.2 mg) and rose bengal (10 μM final concentration) were dissolved in CD_3OD (0.3 mL) and the UV and ^1H NMR spectra were recorded. The mixture was irradiated using visible light (SONY VPL-EX50 slide projector fitted with a 190 W high-pressure Hg lamp) passed through a 475 nm cut-off filter and the reaction was monitored using spectrophotometry and ^1H NMR spectroscopy for periods of up to 60 min. After 60 min of reaction at room temperature, the mixture was evaporated to dryness and then purified by silica gel CC using EtOAc–*n*-hexane (1:1) as the eluent to afford a pure product (0.4 mg), which was identified as ashitabaol B (**1**) on the basis of its UV and ^1H NMR spectra and co-HPLC analysis. ECD (MeOH) $\Delta\varepsilon_{268}$ +38.8; (+)HRESITOFMS *m/z* 209.1165 $[M+H]^+$ (calcd for $C_{12}H_{17}O_3^+$, 209.1172).

*4.16. Conversion of **4** into **2**.*

Oxidation of **4** with Fenton's reagent was performed using a literature method (Manini et al., 2006; Kugelmann et al., 2011) with slight modification. Briefly, to a solution of compound **4** (10 mg) in 2-PrOH (3 mL) were added a solution of $Fe(NH_4)_2(SO_4)_2/6H_2O$ (34 mg) in H_2O (2 mL) and 0.6% H_2O_2 (0.49 mL) at 0 ˚C and the resulting mixture was stirred at room temperature in the dark for 2 h. After evaporation of the solvent, the residue was fractionated by silica gel

CC using EtOAc–*n*-hexane (0:100 to 100:0) as the eluent to afford a product fraction (1.2 mg) together with unreacted **4** (1.2 mg). The product fraction was purified by ODS CC using acetone–H_2O (1:1) as the eluent to afford a pure product (0.6 mg), which was identified as ashitabaol C (**2**) on the basis of its UV and ^{1}H NMR spectra. $[\alpha]_D^{25}$ –20˚ (*c* 0.06, $CHCl_3$) ; ECD (MeOH) $\Delta\varepsilon_{233}$ +0.20, $\Delta\varepsilon_{321}$ –0.03; (+)HRESIFTMS *m/z* 291.1568 $[M+Na]^+$ (calcd for $C_{15}H_{24}O_4Na^+$, 291.1567).

*4.17. Conversion of **5** into **3**.*

Oxidation of **5** was performed in a manner similar to that used to convert **4** into **2** described above with slight modification. To a solution of **5** (1 mg) in 2-PrOH (0.4 mL) were added a solution of $Fe(NH_4)_2(SO_4)_2/6H_2O$ (39 mg) in H_2O (0.4 mL) and 0.5% H_2O_2 (0.68 mL) at –20 ˚C and the resulting mixture was stirred at –20 ˚C in the dark for 2 h. After evaporation of the solvent, the residue was fractionated by silica gel CC using acetone–*n*-hexane (0:100 to 20:80) as the eluent to afford a product (0.4 mg), which was identified as ashitabaol D (**3**) on the basis of its UV and ^{1}H NMR spectra. $[\alpha]_D^{25}$ –143˚ (*c* 0.01, $CHCl_3$); ECD ($CHCl_3$) $\Delta\varepsilon_{327}$ –1.09; (+)HRESIFTMS *m/z* 305.1361 $[M+Na]^+$ (calcd for $C_{15}H_{22}O_5Na^+$, 305.1359).

Acknowledgements

The authors thank Dr. Hyuma Masu (Center for Analytical Instrumentation, Chiba University, Japan) for X-ray crystallographic analysis. This work was supported in part by JSPS KAKENHI Grant Number 18K05335. We thank Editage (http://www.editage.jp) for English language editing.

Appendix A. Supplementary data

Supplementary data associated with this article can be found, in the online version, at http://.

References

Agon, V.V., Bubb, W.A., Wright, A., Hawkins, C.L., Davies, M.J., 2006. Sensitizer-mediated photooxidation of histidine residues: Evidence for the formation of reactive side-chain peroxides. Free Radical Biol. Med. 40, 698–710.

Aoki, N., Ohta, S., 2010. Ashitabaol A, a new antioxidative sesquiterpenoid from seeds of *Angelica keiskei*. Tetrahedron Lett. 51, 3449–3450.

Bae, K.H., Ji, J.M., Kang, J.S., Ahn, B.Z., 1994. A cytotoxic component from Angelicae Koreanae Radix against L1210 and HL-60 cells. Arch. Pharm. Res. 17, 45–47.

Bailly, C., El-Maarouf-Bouteau, H., Corbineau, F., 2008. From intracellular signaling networks to cell death: the dual role of reactive oxygen species in seed physiology. C. R. Biologies 331, 806–814.

Bathe, U., Tissier, A., 2019. Cytochrome P450 enzymes: A driving force of plant diterpene diversity. Phytochemistry 161, 149–162.

Benz, G., Abivardi, C., Muckensturm, B., 1989. Antifeedant activity of bisabolangelone and its analogs against larvae of *Pieris brassicae*. Entomol. Exp. Appl. 53, 257–265.

Chen, J.C., Chiu, M. H., Nie, R.L., Cordell, G.A., Qiu, S.X., 2005. Cucurbitacins and cucurbitane glycosides. Structures and biological activities. Nat. Prod. Rep. 22, 386–399.

Clennan, E.L., 1991. Synthetic and mechanistic aspects of 1,3-diene photooxidation. Tetrahedron 47, 1343–1382.

Dezvarei, S., Lee, J.H.Z., Bell, S.G., 2018. Stereoselective hydroxylation of isophorone by variants of the cytochromes P450 CYP102A1 and CYP101A1. Enzyme Microb. Technol. 111, 29–37.

Fraga, B.M., 2013. Natural sesquiterpenoids. Nat. Prod. Rep. 30, 1226–1264, and previous reviews in the series.

Fry, S.C., 1998. Oxidative scission of plant cell wall polysaccharides by ascorbate induced hydroxyl radicals. Biochem. J. 332, 507–515.

Gesell, A.; Blaukopf, M., Madilao, L., Yuen, M.M.S., Withers, S.G., Mattsson, J., Russell, J.H., Bohlmann, J., 2015. The gymnosperm cytochrome P450 CYP750B1 catalyzes stereospecific monoterpene hydroxylation of (+)-sabinene in thujone biosynthesis in western redcedar. Plant Physiol. 168, 94–106.

Gollnick, K.; Griesbeck, A., 1984. Interactions of singlet oxygen with 2,5-dimethyl-2,4-hexadiene in polar ano non-polar solvents evidence for a vinylog ene-reaction. Tetrahedron 40, 3235–3250.

Graziose, R., Grace, M.H., Rathinasabapathy, T., Rojas-Silva, P., Dekock, C., Poulev, A., Lila, M.A., Smith, P. Raskin, I., 2013. Antiplasmodial activity of cucurbitacin glycosides from *Datisca glomerata* (C. Presl) Baill. Phytochemistry 87, 78–85.

Guedes, A.C., Amaro, H.M., Giao, M.S., Malcata, F.X., 2013. Optimization of ABTS radical cation assay specifically for determination of antioxidant capacity of intracellular extracts of microalgae and cyanobacteria. Food Chem. 138, 638–643.

Jung, H.W., Mahesh, R., Park, J.H., Boo, Y.C., Park, K.M., Park, Y.-K., 2010. Bisabolangelone isolated from *Ostericum koreanum* inhibits the production of inflammatory mediators by down-regulation of NF-κB and ERK MAP kinase activity in LPS-stimulated RAW264.7 cells. Int. Immunopharmacol. 10, 155–162.

Kang, S.W., Kim, H.K., Lee, W.J., Ahn, Y.J., 2006. Toxicity of bisabolangelone from *Ostericum koreanum* roots to *Dermatophagoides farinae* and *Dermatophagoides pteronyssinus* (Acari: Pyroglyphidae). J. Agric. Food Chem. 54, 3547–3550.

Karkonen, A., Kuchitsu, K., 2015. Fenton's oxidation: a tool for the investigation of potential drug metabolites. Phytochemistry 112, 22–32.

Kim, H.S., Lee, Y.J., Lee, H.K., Kim, J.S., Park, Y., Kang, J.S., Hwang, B.Y., Hong, J.T., Kim, Y., Han, S.-B., 2013. Bisabolangelone inhibits dendritic cell functions by blocking MAPK and NF-κB signaling. Food Chem. Toxicol. 59, 26–33.

Knox, J.P.; Dodge, A.D., 1985. Singlet oxygen and plants. Phytochemistry 24, 889–896.

Kuchitsu, K., Kosaka, H., Shiga, T., Shibuya, N., 1995. EPR evidence of generation of hydroxyl radical triggered by N-acetylchitooligosaccharide elicitor and protein phosphatase inhibitor in suspension-cultured rice cells. Protoplasma 188, 138–142.

Kugelmann, E., Albert, C.R., Bringmann, G., Holzgrabe, U., 2011. Fenton's oxidation: a tool for the investigation of potential drug metabolites. J. Pharm. Biomed. Anal. 54, 1047–1058.

Lee, J.W., Yun, C.-Y., Roh, E., Lee, C., Jin, Q., Bang, K.K., Jung, S.-H., Lee, D., Lee, M.K., Kim, Y., Hwang, B.Y., 2012. Melanogenesis inhibitory bisabolane-type sesquiterpenoids from the roots of *Angelica koreana*. Bioorg. Med. Chem. Lett. 22, 2927–2931.

Liszkay, A., Kenk, B., Schopfer, P., 2003. Evidence for the involvement of cell wall peroxidase in the generation of hydroxyl radicals mediating extension growth. Planta 217, 658–667.

Lopez-Amoros, M.L., Hernandez, T., Estrella, I., 2006. Effect of germination on legume phenolic compounds and their antioxidant activity. J. Food Comp. Anal. 19, 277–283.

Luo, H.-J., Wang, J.-Z., Deng, W.-Q., Huang, N-Y., Zou, K., 2012. Bisabolangelone, a gastric H^+/K^+-ATPase inhibitor: homology modeling and docking study. Med. Chem. Res. 21, 2476–2479.

Mak, P.J., Denisov, I.G., 2018. Spectroscopic studies of the cytochrome P450 reaction mechanisms. BBA – Proteins and Proteomics 1866, 178–204.

Manini, P., Briganti, S., Fabbri, C., Picardo, M., Napolitano, A., d'Ischia, M., 2006. Free radical oxidation of 15-(*S*)-hydroxyeicosatetraenoic acid with the Fenton regent: characterization of an epoxy-alcohol and cytotoxic 4-hydroxy-2*E*-nonenal from the heptatrienyl radical pathway. Chem. Phys. Lipids 142, 14–22.

Matsumoto, M.; Dobashi, S.; Kuroda, K.; Kondo, K., 1985. Sensitized photo-oxygenation of acyclic conjugated dienes. Tetrahedron 41, 2147–2154.

Melera, A., Gut, M., Noller, C.R., 1960. Structure of cucurbitacin B. Tetrahedron Lett. 13–18.

Muckensturm, B., Duplay, D., Robert, P.C., Simonis, M.T., Kienlen, J.-C., 1981. Substances antiappetantes pour insectes phytophages presentes dans *Angelica silvestris* et *Heracleum sphondylium*. Biochem. Syst. Ecol. 9, 289–292.

Murthy, R.S.; Bio, M.; You, Y., 2009. Low energy light-triggered oxidative cleavage of olefins. Tetrahedron Lett. 50, 1041–1044.

Nawrot, J., Harmatha, J., Novotny, L., 1984. Insect feeding deterrent activity of bisabolangelone and of some sesquiterpenes of eremophilane type. Biochem. Syst. Ecol. 12, 99–101.

Novotny, L., Samek, Z., Sorm, F., 1966. Structure of bisabolangelone, a sesquiterpenic oxo alcohol from Angelica sylvestris. Tetrahedron Lett. 3541–3546.

Parsons, S., Flack, H., 2004. Precise absolute-structure determination in light-atom crystals. Acta Cryst. A60, s61.

Parsons, S., Flack, H.D., Wagner, T., 2013. Use of intensity quotients and differences in absolute structure refinement. Acta Cryst. B69, 249–259.

Riss, B.; Garreau, M.; Fricero, P.; Podsiadly, P.; Berton, N.; Buchter, S., 2017. Total synthesis of TMS-*ent*-bisabolangelone. Tetrahedron 73, 3202–3212.

Riss, B., Muckensturm, B., 1989. Synthese totale de la (±) bisabolangelone (1). Tetrahedron 45, 2591–2604.

Schopfer, P., Plachy, C., Frahry, G., 2001. Production of reactive oxygen intermediates (superoxide radicals, hydrogen peroxide, and hydroxyl radicals) and peroxidase in germinating radish seeds controlled by light, gibberellin, and abscisic acid. Plant Physiol. 125, 1591–1602.

Schweikert, C., Liszkay, A., Schopfer, P., 2000. Scission of polysaccharides by peroxidese-generated hydroxyl radicals. Phytochemistry 53, 565–570.

Schweikert, C., Liszkay, A., Schopfer, P., 2002. Polysaccharide degradation by Fenton reaction- or peroxidase-generated hydroxyl radicals in isolated plant cell walls. Phytochemistry 61, 31–35.

Sheldrick, G.M., 1997. *SHELXS-97*: Program for Crystal Structure Solution. University of Göttingen, Göttingen, Germany.

Sheldrick, G.M., 2013. *SHELXL-2013*: Program for Crystal Structure Refinement. University of Göttingen, Göttingen, Germany.

Sheldrick, G.M., 2014. *SHELXL-2014/6*: Program for Crystal Structure Refinement. University of Göttingen, Göttingen, Germany.

Tabata, H., Katsube, T., Moriya, K., Utsumi, T., Yamasaki, Y., 2010. Protective activity of components of an edible plant, Mallotus japonicus, against oxidative modification of proteins and lipids. Food Chemistry 118, 548–553.

Wang, J., Zhu, L., Zou, K., Cheng, F., Dan, F., Guo, Z., Cai, Z., Yang, J., 2009. The anti-ulcer activities of bisabolangelone from *Angelica polymorpha*. J. Ethnopharmacol. 123, 343–346.

Yu, D.Q., Chen, R.Y., Xie, F.Z., 1995. Structure elucidation of ligustilone from *Ligusticum sinensis* Oliv. Chi. Chem. Lett. 6, 391–394.

Yu, F., Xu, D., Lei, R., Li, N., Li, K., 2008. Free-radical scavenging capacity using the Fenton reaction with rhodamine B as the spectrophotometric

indicator. J. Agric. Food Chem., 56, 730–735.

Zhu, F., Cai, Y., Sun, M., Ke, J., Lu, D., Corke, H., 2009. Comparison of major phenolic constituents and in vitro antioxidant activity of diverse Kudingcha genotypes from *Ilex kudingcha*, *Ilex cornuta*, and *Ligustum robustum*. J. Agric. Food Chem. 57, 6082–6089.

Zhu, N., Sun, Z., Hu, M., Li, Y., Zhang, D., Wu, H., Tian, Y., Li, P., Yang, J., Ma, G., Xu, X., 2018. Cucurbitane-type triterpenes from the tubers of *Hemsleya penxianensis* and their bioactive activity. Phytochemistry 147, 49–56.

Table 1

NMR spectroscopic data for **1**–**3**.

No.	**1**[a]		**2**[a]		**3**[a]	
	δ_H (*J* in Hz)	δ_C	δ_H (*J* in Hz)	δ_C	δ_H (*J* in Hz)	δ_C
1	4.77 (br t, 4.6)	79.2	5.36 (ddd, 10.1, 2.4, 1.2)	128.5		199.0
2	5.72 (br s)	116.9	5.78 (ddd, 10.1, 2.4, 1.2)	136.4	5.97 (br s)	125.6
3		144.5		66.7		161.2
4α	2.00 (br d, 13.4)	28.7	1.86 (br d, 14.6)	36.6	2.60 (br d, 18.3)	40.4
4β	2.09 (br dd, 13.4, 11.6)		1.55 (ddd, 14.6, 13.1, 3.7)		2.67 (dd, 18.3, 2.7)	
5α	1.19 (dddd, 13.4, 12.8, 11.6, 5.2)	19.0	1.72 (dddd, 16.2, 13.1, 10.1, 2.7)	19.0	4.52 (q, 2.7)	66.3
5β	1.89 (dddd, 12.8, 4.6, 4.6, 2.1)		1.85 (m)			
6	2.07 (ddd, 13.4, 4.6, 4.6)	44.7	2.48 (ddd, 10.1, 5.2, 2.4)	42.7	2.84 (d, 2.7)	62.7
7		80.6		79.6		80.3
8		181.1		202.7		207.1
9	5.31 (d, 8.5)	99.1	6.69 (d, 15.3)	119.0	7.19 (d, 15.6)	119.7
10	9.89 (d, 8.5)	189.4	7.16 (d, 15.3)	155.9	7.11 (d, 15.6)	156.7
11	1.56 (3H, s)	26.7		71.2		71.3
12	1.81 (3H, br s)	23.7	1.38 (3H, s)	29.3	1.40 (3H, s)	29.2
13			1.39 (3H, s)	29.5	1.41 (3H, s)	29.3
14			1.40 (3H, s)	22.5	1.43 (3H, s)	22.4
15			1.27 (3H, s)	29.2	2.03 (3H, br s)	24.8

[a] Chemical shifts were measured in $CDCl_3$ at 400 MHz for ^1H, 100 MHz for ^{13}C.

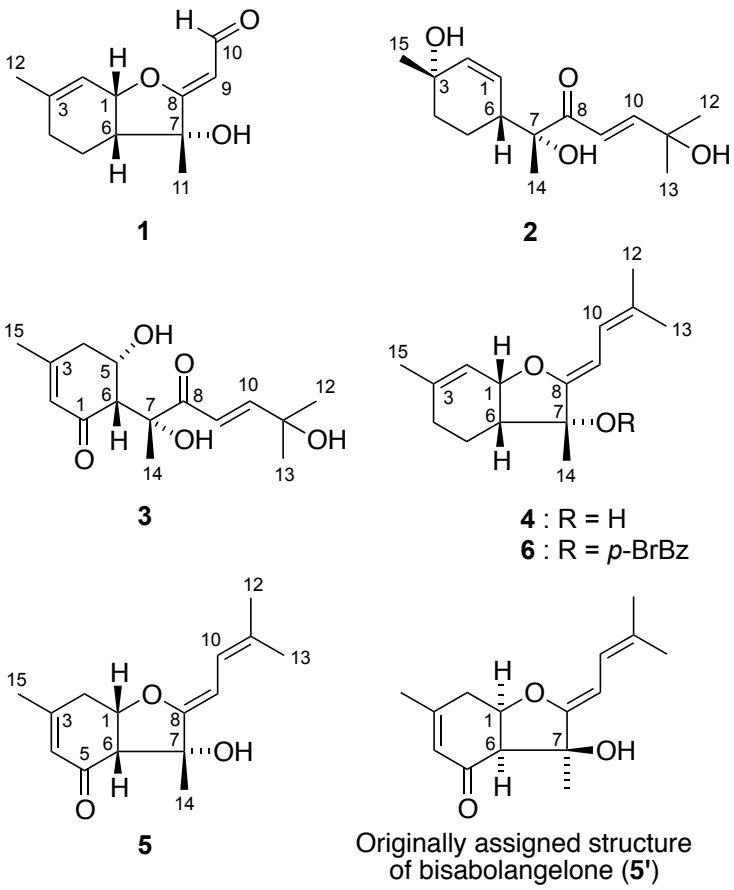

Fig. 1. Structures of compounds **1**–**6**.

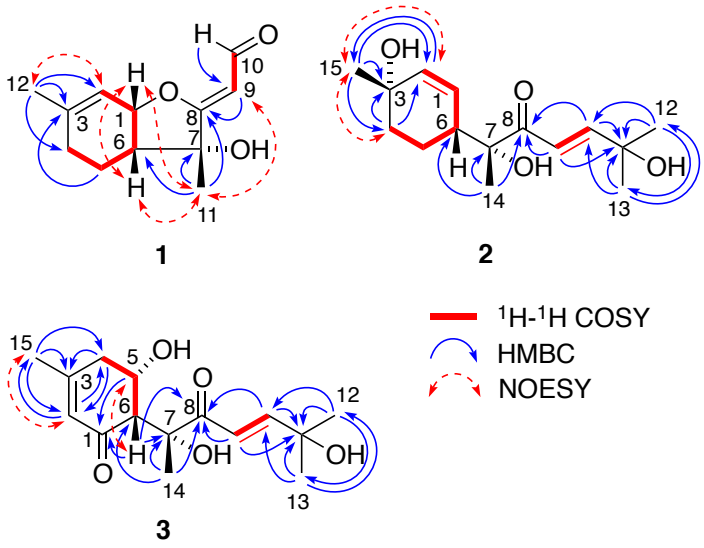

Fig. 2. ^{1}H–^{1}H COSY, HMBC, and NOESY key data for **1**–**3**.

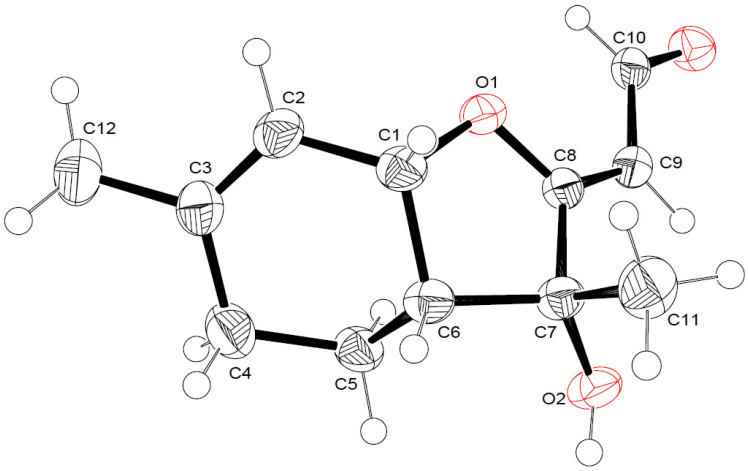

1

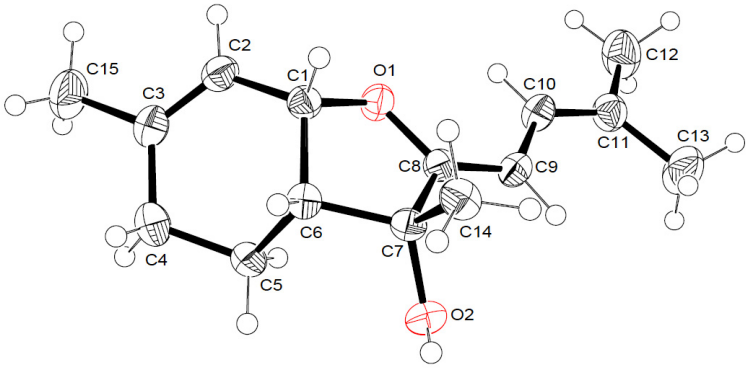

4

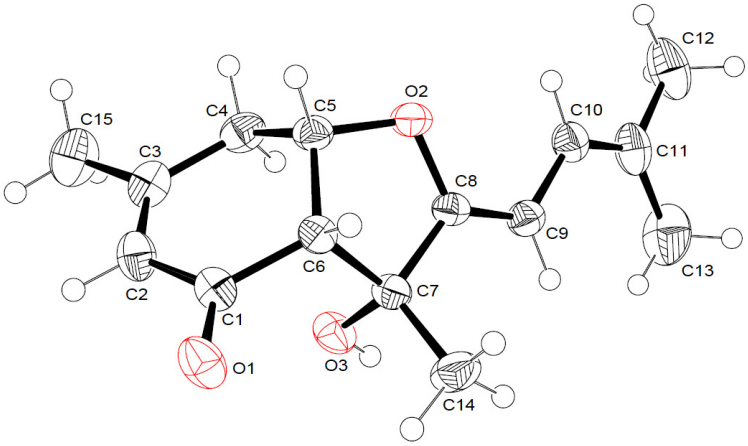

5

Fig. 3. ORTEP diagrams of **1**, **4**, and **5**.

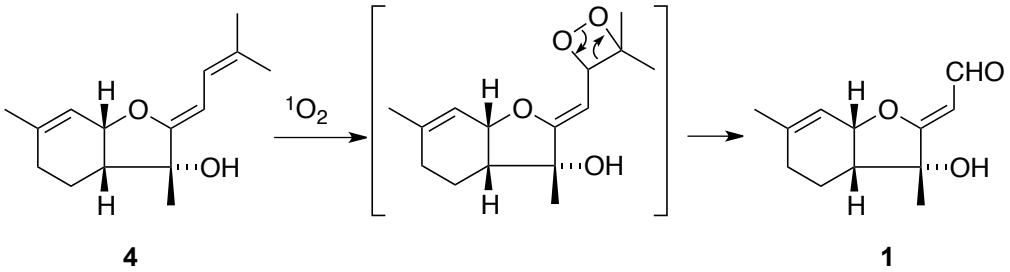

4 **1**

Fig. 4. Possible oxidation pathway from **4** to **1** by singlet oxygen through a dioxetane intermediate.

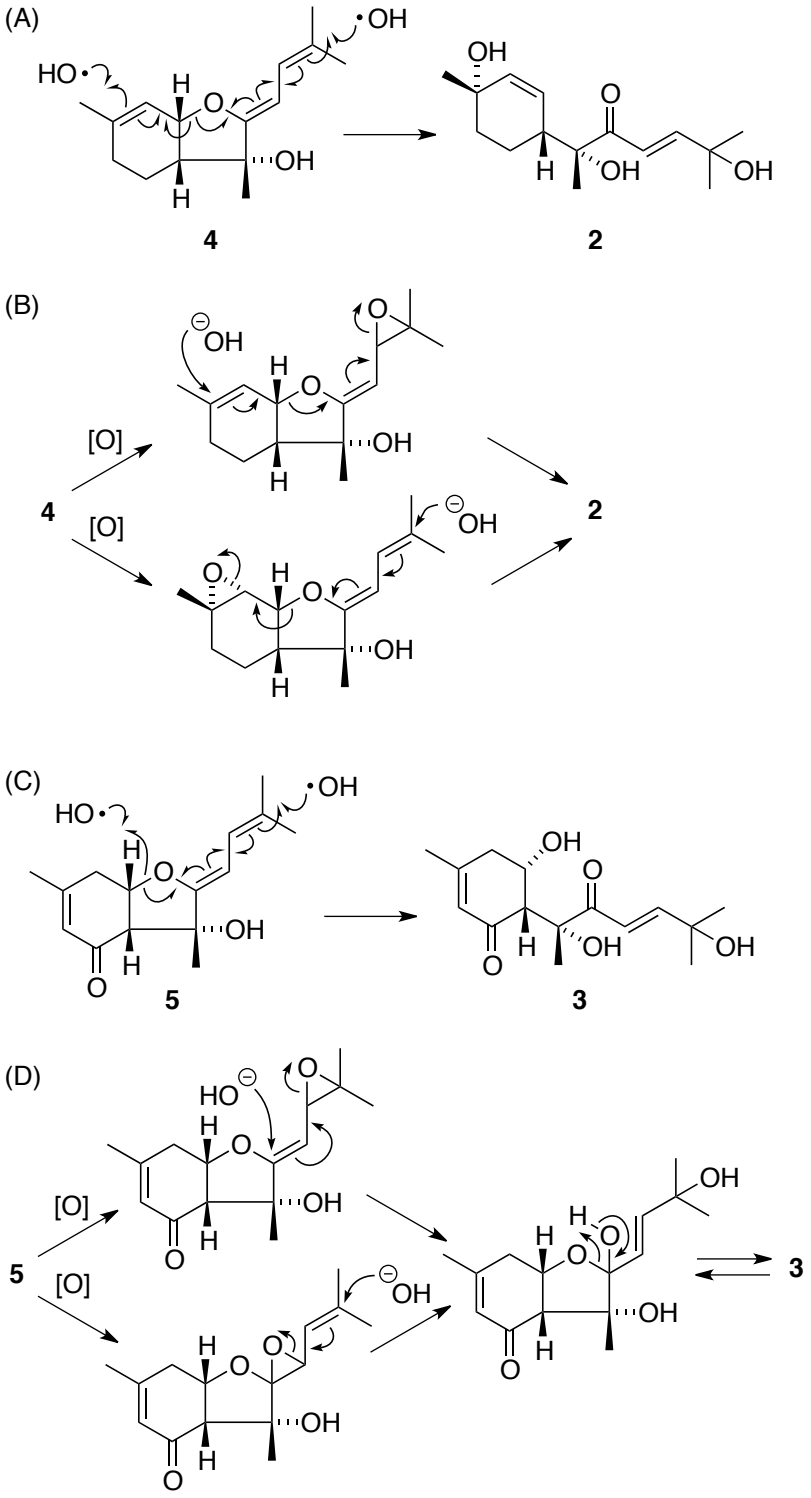

Fig. 5. Possible pathways from **4** to **2** (A and B) and from **5** to **3** (C and D) by hydroxyl radicals (A and C) and via an epoxide intermediate (B and D).